RAPID COMMUNICATIONS

PHYSICAL REVIEW B VOLUME 28, NUMBER 11 1 DECEMBER 1983

Rapid Communications

The Rapid Communications section is intended for the accelerated publication of important new results. Manuscripts submitted to this section are given priority in handling in the editorial office and in production. A Rapid Communication may be no longer than 3½ printed pages and must be accompanied by an abstract. Page proofs are sent to authors, but, because of the rapid publication schedule, publication is not delayed for receipt of corrections unless requested by the author.

Excitation phenomena and line intensities in high-resolution NMR powder spectra of half-integer quadrupolar nuclei

A. Samoson and E. Lippmaa
Institute of Chemical Physics and Biophysics of the Estonian Academy of Sciences,
Tallinn 200 001, Union of Soviet Socialist Republics

(Received 1 August 1983)

A theoretical analysis of the general excitation phenomena of half-integer $I > \frac{1}{2}$ nuclear spins in a strong radio-frequency field shows that coherence between the affected spin states leads to complicated time behavior of the total nuclear magnetization. Very short excitation pulses lead to quantitatively useful high-resolution NMR spectra of quadrupolar nuclei in powder samples spun at the magic angle, while selective spin-state time development during longer rf pulses permits the use of two-dimensional Fourier-transform NMR techniques with simultaneous measurement of the isotropic chemical shifts and the corresponding quadrupole interaction parameters.

Recently there has been a surge of interest in the powder spectra of spin $I = \frac{3}{2}$ and $\frac{5}{2}$ nuclei, particularly those of sodium ^{23}Na and aluminum ^{27}Al. The magic angle spinning (MAS) technique[1] has proved to be quite effective in enhancing the spectral resolution of the central $(\frac{1}{2} \leftrightarrow -\frac{1}{2})$ transition line shape, thus providing a means for measuring the main components of the quadrupole interaction tensors together with the isotropic screening values.[2,3] Other rotation angles, used in the variable angle sample spinning technique,[4] can provide single-peaked line shapes, but without the benefit of averaging the chemical shift anisotropy and dipole-dipole couplings, and with both the peak and the line center of gravity shifted far from the isotropic screening value. Many of the chemical shifts measured at present are not the true isotropic shifts but rather represent the centers of gravity of line shapes of uncertain origin that contain a considerable field-dependent quadrupolar share. The line intensities are generally in a poor correlation with the number of quadrupolar nuclei involved. Measurements at different magnetic field strengths would help but are impractical as a result of unfavorable ω_Q/ω_L ratios and severe line broadening at lower fields.

We have found that detailed knowledge of the excitation process of half-integer spins in a powder sample spun at the magic angle in a constant strong magnetic field can provide new insights into the problems of high-resolution NMR spectroscopy of these nuclei. Time development of the spin states under the joint influence of Zeeman and quadrupole interactions in a strong resonant transverse radio-frequency (rf) field provides both the excitation necessary for NMR spectrum registration and, through a second Fourier transform, some information about the quadrupolar interaction tensor components.

Consider a quadrupolar nucleus in a strong static magnetic field B_z, subjected to quadrupole interaction such that

$$|\mathscr{H}_Z| >> \mathscr{H}_Q| \;,$$

and to a strong resonant transverse rf field with an amplitude $2\gamma B_{\mathrm{rf}} = 2\omega_{\mathrm{rf}}$. Under the conditions of MAS-NMR and, if needed, high power dipolar decoupling, we can ignore all other intereactions and use only the secular part of the quadrupole interaction Hamiltonian. The time-independent secular part of the spin Hamiltonian during the rf pulse in the interaction representation is formed as the average Hamiltonian over the Larmor period in the zeroth approximation of the average Hamiltonian theory[5]:

$$\bar{\bar{\mathscr{H}}}_P = \bar{\bar{\mathscr{H}}}_Q^{(0)} + \bar{\bar{\mathscr{H}}}_{\mathrm{rf}}^{(0)} = \omega_Q(3I_z^2 - I^2) - \omega_{\mathrm{rf}} I_x \;, \tag{1}$$

where the magnitude of the quadrupolar term

$$\omega_Q = \frac{eQV_{20}\sqrt{2/3}}{4I(2I-1)\hbar}$$

is a function of the electric-field-gradient (EFG) tensor with the principal values $\rho_{20} = \sqrt{3/2}eq$ and $\rho_{2\,\pm 2} = \frac{1}{2}eq\eta$.

The interaction tensor components

$$V_{2j} = \sum_{m'} D_{m'j}^{(2)}(\omega_r t, \arccos\sqrt{1/3}, 0) \sum_{m''} D_{m''m'}^{(2)}(\alpha,\beta,\gamma)\rho_{2m''}$$

are expressed through the Wigner rotation matrices $D_{k1}^{(2)}$ containing two sets of Eulerian angles that define the orientation of B_z relative to the spinner frame rotating with rate $\omega_r/2\pi$ (Hz), at the magic angle 54°44′ to the applied static magnetic field, and the orientation of the spinner frame with respect to the principal axes system of the EFG tensor in any single crystal in the powder sample. The actual values of ω_Q vary widely with the orientation of crystals during sample spinning. If $\omega_{\mathrm{rf}} << \omega_Q$, then only the central $(\frac{1}{2} \leftrightarrow -\frac{1}{2})$ transition can be excited by the rf pulse and the corresponding Rabi frequency is $(I+\frac{1}{2})\omega_{\mathrm{rf}}$.[6] In the opposite case $\omega_{\mathrm{rf}} >> \omega_Q$, all spin states develop coherence, and the total transverse magnetization oscillates at ω_{rf} during the rf pulse (see Fig. 1). The experimentally more realistic in-

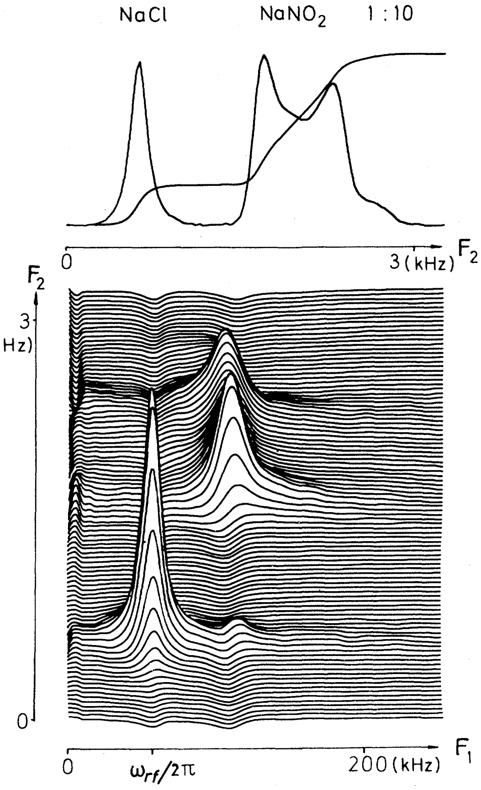

FIG. 1. Upper figure shows 1:4 signal intensities ratio in 52.9-MHz ^{23}Na MAS-NMR spectrum of a 1:10 molar mixture of solid NaCl and $NaNO_2$. In the 2D representation (lower figure) the F_1 axis shows the Fourier components of the transverse magnetization oscillating under the influence of a strong $\omega_{\rm rf}/2\pi = 55$ kHz resonant radio-frequency field. The main component of $NaNO_2$ oscillation corresponds to a Rabi frequency of $(I+\frac{1}{2})\omega_{\rm rf}$ and the spectral features at zero oscillation frequency are artifacts caused by spectrometer electronics. The chemical shifts and line shapes are displayed along the F_2 axis.

termediate values of ω_Q lead to an aperiodic behavior of the central transition transverse magnetization described by the time development of the density matrix $\tilde{\rho}(t_p)$ under the influence of $\bar{\bar{\mathscr{H}}}_P$ during the time t_P that the rf pulse is switched on.

This time development may be calculated by diagonalizing $\bar{\bar{\mathscr{H}}}_P$ and performing the corresponding orthogonal transformations on $\tilde{\rho}(0)$ and operators of the observables. However, as a result of possible large variations of ω_Q relative to $\omega_{\rm rf}$, such expressions lack clarity in describing the excitation processes. In case of short excitation pulses $\omega_{\rm rf} t_P = \phi << 1$, the most transparent analytical results follow from a recurrent expansion of the density matrix

$$\tilde{\rho}(t_P) = [0] + \frac{1}{1!}[1] + \frac{1}{2!}[2] + \cdots + \frac{1}{n!}[n] + \cdots \quad , \qquad (2)$$

where $[0] = \tilde{\rho}_0$ and

$$[n+1] = \sum_{k',r',s'} a^{r's'}_{n+1,k'} I^{r's'}_{k'}$$

$$= \sum_{\substack{k,r,s\\k',r',s'}} G_{k'r's'krs} a^{rs}_{nk} I^{rs}_{k} = [-i\bar{\bar{\mathscr{H}}}_P t_P, [n]] \quad . \qquad (3)$$

This expression defines the matrix of commutation relationships G used in the recurrent expansion (2). Use of the single transition $(r \leftrightarrow s)$ fictitious spin operators $I^{rs}_{k=x,y,z}$ due to Wokaun and Ernst,[7] which are defined in the basis of eigenfunctions $|j\rangle = |I-j+1\rangle$, $j = 1, \ldots, 2I+1$ in the following way:

$$\langle i | I^{rs}_x | j \rangle = \tfrac{1}{2}(\delta_{ir}\delta_{js} + \delta_{is}\delta_{jr}) \quad ,$$

$$\langle i | I^{rs}_y | j \rangle = \frac{i}{2}(-\delta_{ir}\delta_{js} + \delta_{is}\delta_{jr}) \quad ,$$

$$\langle i | I^{rs}_z | j \rangle = \tfrac{1}{2}(\delta_{ir}\delta_{js} - \delta_{is}\delta_{jr}) \quad ,$$

allowed to linearize $\bar{\bar{\mathscr{H}}}_P$, and led to a convenient linear expression (3) for the evaluation of next higher terms in the recurrent expansion (2)

$$[n+1] = \sum_{u} a^{u}_{n+1} I^{u} = \sum_{u,v} G_{uv} a^{v}_{n} I^{v} \quad . \qquad (4)$$

Because of the symmetry properties of the Hamiltonian (1), only a limited number of independent linear combinations I^u, I^v of the fictitious spin operators appear in the summations in (4). For $I = \frac{3}{2}$, $I^1 = I^{12}_x - I^{34}_x$, $I^2 = I^{13}_x - I^{24}_x$, $I_3 = I^{12}_z + I^{34}_z$, $I^4 = I^{23}_z$, $I^5 = I^{12}_y + I^{34}_y$, $I^6 = I^{13}_y + I^{24}_y$, $I^7 = I^{23}_y$, $I^8 = I^{14}_y$, the equilibrium density matrix is represented by the coefficients

$$a^{u \neq 3,4}_0 = 0 \quad , \quad a^3_0 = 3b, \quad a^4_0 = 4b, \quad b = -\omega_L/kT \quad ,$$

and the commutation relationships are represented by the matrix of G_{uv}:

$$\underline{G} = \begin{pmatrix} \underline{0} & \underline{G}'' \\ \underline{G}' & \underline{0} \end{pmatrix} \quad ,$$

$$\underline{G}' = \begin{pmatrix} \psi & \phi & \sqrt{3}\phi & -\frac{\sqrt{3}}{2}\phi \\ \phi & \psi & 0 & 0 \\ 0 & -\sqrt{3}\phi & -2\phi & 2\phi \\ 0 & \sqrt{3}\phi & 0 & 0 \end{pmatrix} \quad ,$$

$$\underline{G}'' = \begin{pmatrix} -\psi & -\phi & 0 & 0 \\ -\phi & -\psi & \frac{\sqrt{3}}{2}\phi & -\frac{\sqrt{3}}{2}\phi \\ -\sqrt{3}\phi & 0 & 0 & 0 \\ 0 & 0 & -2\phi & 0 \end{pmatrix} \quad ,$$

and $\psi = 6\omega_Q t_P$.

By limiting the highest power of ϕ one can disregard most of the $\underline{G}$ matrix elements beginning with a certain value of n and arrive at easily summable expansion coefficients for the operator of interest. The NMR signal generated by coherence in the $I = \frac{3}{2}$ spin central transition is proportional to

$$\sum_{n=2I+1}^{\infty} \frac{1}{n!} a^7_n I^7 \quad ,$$

where up to the third power in ϕ, $a^7_1 = 2b\phi$, $a^7_3 = -2b\phi^3$,

$$a^7_n = (-1)^{(n+1)/2} 3(n-1) b\phi^3 \psi^{n-3} \quad (n \geq 5) \quad .$$

Summation yields the central transition NMR signal amplitude as a function $J_1(\psi, \phi)$ of the quadrupolar flip angle ψ and a power series of the rf flip angle ϕ:

$$J_{3/2}(\psi,\phi)\propto b\langle \tfrac{1}{2}|I_y|-\tfrac{1}{2}\rangle\langle -\tfrac{1}{2}|I_y^{23}|\tfrac{1}{2}\rangle \times\left[2\phi+\left(\frac{3(\sin\psi-\psi\cos\psi)}{\psi^3}-\frac{4}{3}\right)\phi^3+\cdots\right], \quad (5)$$

and, for $I=\frac{5}{2}$,

$$J_{5/2}(\psi,\phi)\propto b\langle \tfrac{1}{2}|I_y|-\tfrac{1}{2}\rangle\langle -\tfrac{1}{2}|I_y^{34}|\tfrac{1}{2}\rangle \times\left[3\phi+\left(\frac{12(\sin\psi-\psi\cos\psi)}{\psi^3}-\frac{9}{2}\right)\phi^3+\cdots\right]. \quad (6)$$

The fictitious spin operators I_y^{23} and I_y^{34} correspond to the central ($\frac{1}{2}\leftrightarrow -\frac{1}{2}$) transitions and

$$I_y=\sqrt{3}(I_y^{12}+I_y^{34})+2I_y^{23}\ \text{for}\ I=\tfrac{3}{2}\ ,$$

$$I_y=\sqrt{5}(I_y^{12}+I_y^{56})+2\sqrt{2}(I_y^{23}+I_y^{45})+3I_y^{34}\ \text{for}\ I=\tfrac{5}{2}\ .$$

It is immediately apparent that if the rf flip angle is small, $\phi^3 << 1$, then the central transition signal intensity is proportional to $|\langle\frac{1}{2}|I_y|-\frac{1}{2}\rangle|^2 b\phi$, but independent of the magnitude of ω_Q. It can be readily proven that the formulas (5) and (6) lead, in the case of extremely large and infinitely small quadrupole interaction constants, to results consistent with the transverse magnetization oscillation frequencies $(I+\frac{1}{2})\omega_{\rm rf}$ and $\omega_{\rm rf}$, respectively. All intermediate oscillation frequencies are also possible, but higher frequencies have very low intensities.

The central transition NMR frequency can be calculated by forming an effective Hamiltonian

$$\tilde{\mathscr{H}}^{\rm eff}=\bar{\tilde{\mathscr{H}}}_Q^{(0)}-\frac{i\omega_L}{4\pi}\int_0^{2\pi/\omega_L}dt\int_0^t[\tilde{\mathscr{H}}_Q(t),\tilde{\mathscr{H}}_Q(t')]dt' \quad (7)$$

as the average Hamiltonian over the Larmor period in the first approximation of the average Hamiltonian theory. The strong radio-frequency field is turned off during registration of the free-induction decay, and the nondiagonal matrix elements caused by the full quadrupole Hamiltonian

$$\tilde{\mathscr{H}}_Q(t)=\bar{\tilde{\mathscr{H}}}_Q^{(0)}+\frac{eQ/\hbar}{4I(2I-1)}[-V_{21}(I_-I_z+I_zI_-)e^{-i\omega_L t}+V_{2-1}(I_+I_z+I_zI_+)e^{+i\omega_L t}+V_{22}I_-^2e^{-2i\omega_L t}+V_{2-2}I_+^2e^{+2i\omega_L t}]$$

can no longer be ignored. However, for most half-integer spins in strong magnetic fields $\omega_L \geqslant 10\omega_Q$, and $\tilde{\mathscr{H}}^{\rm eff}$ is diagonal in the basis of Zeeman Hamiltonian eigenfunctions to a precision better than that provided by the first approximation of the average Hamiltonian theory.[2] All the nondiagonal matrix elements are either zero or $eQV_{2i}/\hbar\omega_L$ times smaller than differences between the respective diagonal elements for all possible single-crystal orientations in the powder sample.

Sample spinning provides slow ($\omega_r << \omega_L$) parametric modulation of the orientation-defining angles ($\gamma+\omega_r t$) in the expression for the interaction tensor components V_{2j}, and the registered line shape $J(\omega)$ can be derived as the sum of line intensities corresponding to any particular range of the $\tilde{\mathscr{H}}^{\rm eff}$ central transition frequencies $\bar{\omega}(\alpha,\beta)$, averaged over the rotation period ω_r^{-1}.[2,3] These line shapes can best be calculated according to Haeberlen[8] from an integral equation where the line intensity between arbitrary frequency limits ω_a, ω_b is equaled to the statistically expected number of nuclei resonating between these limits, weighted by their orientation-dependent excitation efficiency $J_I(\psi,\phi)$ calculated from Eqs. (5) and (6). For the line intensity in arbitrary units,

$$\int_{\omega_a}^{\omega_b}J(\omega)\,d\omega=\iint_{\omega_a<\bar{\omega}(\alpha,\beta)<\omega_b}d\alpha\sin\beta\,d\beta\int_0^{2\pi}J_I(\psi,\phi)\,d\gamma\ . \quad (8)$$

This is true as long as the spinner frequency exceeds the total spread of the averaged resonance frequencies $\bar{\omega}(\alpha,\beta)$.

If the excitation pulse is strong ($\omega_{\rm rf} >> \omega_r$) but short ($\phi << 1$), then $J_I(\psi,\phi)$ is independent of the orientation angles, excitation of the central transition is uniform all over the powder sample, and the corresponding MAS-NMR signal is directly proportional to the number of resonating nuclei. In the limit of short radio-frequency pulses this signal is exactly $4I(I+1)/3(I+\frac{1}{2})$ times weaker than that in the otherwise identical $\psi=0$ case, where all the transitions are coherently excited and registered.

^{23}Na MAS-NMR spectra of 1:10 molar ratio mixture of solid polycrystalline NaCl and $NaNO_2$, registered with a very short ($t_p=2\ \mu$s) strong rf excitation pulse, are shown in Fig. 1. The ^{23}Na quadrupolar interaction is very small in NaCl ($e^2qQ/h << \omega_r$), no rotation sidebands are formed, and the line shows its true intensity and a regular inversion behavior due to the practically uniform excitation of all transitions. In the case of larger quadrupole interactions as in solid $NaNO_2$ ($e^2qQ/h = 1.1$ MHz $>> \omega_r/2\pi$; $\eta=0.1$),[9] part of the line intensity coming from other than the central transitions is smeared into innumerable sidebands of very low intensity, and the registered centerband intensity is $\frac{5}{2}$ times smaller than that expected from the mole ratio, but the line shape is undistorted and readily interpretable.

Evaluation of the central transition excitation function $J_I(\psi,\phi)$ in case of long excitation pulses by means of a recurrent expansion becomes impractical, and we performed numerical diagonalization of $\bar{\tilde{\mathscr{H}}}_P$. Differences of eigenvalues of the diagonalized Hamiltonian introduce complicated time dependence into the excitation function at frequencies dependent on first-order quadrupolar shifts of all transitions due to mixing of the original eigenfunctions by the rf pulse. If the rf pulses are still short compared with a MAS period, changes in orientation of the sample during the excitation period can be neglected and the corresponding Hamiltonian regarded as stationary.

For rf pulses up to 9-μs duration, numerically calculated changes in the line shape $J(\omega)$, assuming a stationary Hamiltonian, agree well with the experimental spectra of the $\frac{1}{2}\leftrightarrow -\frac{1}{2}$ transition of ^{55}Mn in polycrystalline $KMnO_4$ (Fig. 2). These line shapes are related to the results of Polak, Highe, and Vaughan,[11] who studied ^{23}Na spectra of a single crystal of sodium β-alumina, where the correlation of first-

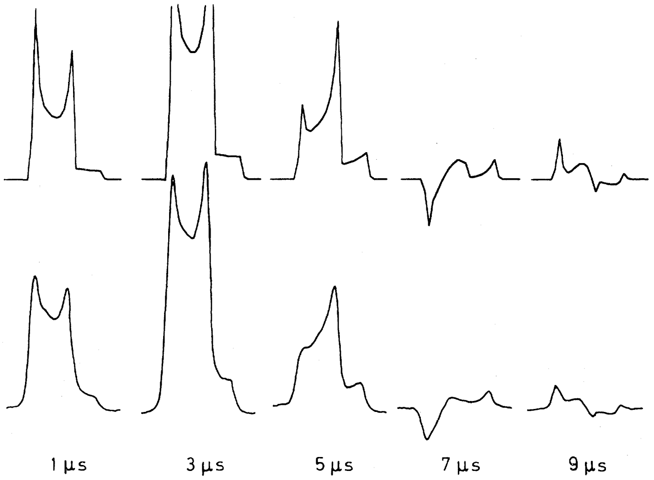

FIG. 2. The upper row shows results of a numerical calculation for $e^2qQ/h = 1.6$ MHz, $\eta = 0$ (Ref. 10), $\omega_{\mathrm{rf}}/2\pi = 48$ kHz; the lower row displayes experimental 49.5-MHz MAS-NMR spectra of ^{55}Mn ($I = \frac{5}{2}$) in polycrystalline $KMnO_4$. All experimental spectra were registered on a Bruker Physik CXP-200 spectrometer at 4.7 T.

and second-order quadrupolar shifts was achieved by means of an additional rf pulse of different frequency. This preparatory pulse affected primarily a $\frac{3}{2} \longleftrightarrow \frac{1}{2}$ transition, and the effect was detected on the central transition due to a common energy level.

Frequency components of the excitation function can be registered by performing a second Fourier transformation over a series of spectra registered with various spin-state development times t_P, increasing the rf pulse length by constant increments. This results in representation of the spectra along two frequency axes (see the lower part of Fig. 1). In NaCl the excitation proceeds nearly exclusively at $\omega_{\mathrm{rf}}/2\pi = 55$ kHz (F_1 axis) with a very small $2\omega_{\mathrm{rf}}$ component due to crystal imperfections and possibly strain during sample spinning; whereas in $NaNO_2$ the excitation spectrum is more complicated, but, due to the relatively large ω_Q, is concentrated on $(I + \frac{1}{2})\omega_{\mathrm{rf}}/2\pi = 110$ kHz. This information is quite separate from the chemical shift information displayed along the F_2 axis. It is obvious that such excitation pulse-length dependences, leading to a new kind of two-dimensional (2D) Fourier-transformed high-resolution NMR spectroscopy in solids, can be used for the evaluation of quadrupolar interaction parameters even in cases where only the powder pattern centers of gravity with no line structure can be measured, thus providing a universal means for correcting the apparent isotropic shielding values and line intensity of quadrupolar nuclei with half-integer spins.

---

[1] E. R. Andrew, A. Bradbury, and R. G. Eades, Arch. Sci. 11, 223 (1958).

[2] E. Kundla, A. Samoson, and E. Lippmaa, Chem. Phys. Lett. 83, 229 (1981).

[3] A. Samoson, E. Kundla, and E. Lippmaa, J. Magn. Reson. 49, 350 (1982).

[4] S. Ganapathy, S. Schramm, and E. Oldfield, J. Chem. Phys. 77, 4360 (1982).

[5] U. Haeberlen and J. S. Waugh, Phys. Rev. 175, 453 (1968).

[6] V. H. Schmidt, Phys. Rev. B 7, 4145 (1973).

[7] A. Wokaun and R. R. Ernst, J. Chem. Phys. 67, 1752 (1977).

[8] U. Haeberlen, *High Resolution NMR in Solids* (Academic, New York, 1976).

[9] A. Weiss, Z. Naturforsch. 15A, 536 (1960).

[10] D. J. Burton and R. K. Harris, J. Chem. Soc. Chem. Commun. p. 256 (1982).

[11] M. Polak, A. J. Highe, and R. W. Vaughan, J. Magn. Reson. 37, 357 (1980).